A comparison between CFD simulations and experiments for predicting the far wake of horizontal axis tidal turbines

M. E. Harrison, W. M. J. Batten, L. E. Myers, A. S. Bahaj

Sustainable Energy Research Group,
School of Civil Engineering and the Environment,
University of Southampton
Southampton, SO17 1BJ, UK
E-mail: m.e.harrison@soton.ac.uk

Abstract

Actuator discs may be used as a simple method for simulating horizontal axis tidal turbines, both in experiments and CFD models. They produce a similar far wake to a real turbine, but eliminate some of the scaling issues which occur in experiments, and reduce the mesh density required in CFD simulations. This paper examines methods for applying a simple actuator disc in a commercial CFD code, Ansys CFX, and compares the wake produced with experimental results for similar values of disk thrust coefficient (C_T). The results show that the CFD model gives reasonable agreement with the experimental results. The main factors affecting the wake structure are the initial C_T value, the ambient turbulence levels, and potentially the disc induced turbulence. The main differences between the models and experiments were in terms of the turbulence levels throughout the model. With further development, it is considered that the CFD actuator disc could be an accurate and validated method for numerically modelling tidal turbines.

Keywords: CFD, tidal current, turbine, wake

Nomenclature

A_d	=	area of the disc/rotor
C_T	=	coefficient of thrust
D	=	turbine/disc diameter
D_h	=	water depth
ε	=	turbulence eddy dissipation
I	=	turbulence intensity
k	=	turbulence kinetic energy
K	=	resistance coefficient of porous material
Δp	=	change in pressure across disc
ρ	=	fluid density
S	=	momentum source
T	=	thrust
U_0	=	free-stream stream-wise fluid velocity
U_d	=	stream-wise fluid velocity at disc
$U_{s(i,j,k)}$	=	superficial fluid velocity in x,y, or z direction
θ	=	open area ratio for a porous material (open area/total area)
Δx_i	=	thickness of porous region (disc)
U_I	=	modelled inlet velocity.
U^*	=	friction velocity
y	=	water depth.
$y+$	=	dimensionless wall distance
ν	=	kinematic viscosity (of water)

1 Introduction

A simple method for simulating the effect of a horizontal axis tidal stream turbine on downstream flow is by simulating it with a porous disc of the same diameter. The porous or actuator disk applies a similar thrust force upon the moving fluid as a set of rotating blades, although turbulence structures shed from the disk vary, compared to a rotor. Experiments utilising actuator disks allow extensive flow mapping studies to be conducted without the requirement for construction of scale turbines or the cost associated with large experimental test facilities. Extensive wake experiments using this methodology have been carried out at the University of Southampton [1].

Reynolds Averaged Navier-Stokes (RANS) Computational Fluid Dynamics (CFD) models are now being implemented to utilise these results and scale-up the experimental scenarios to understand wake effects in tidal stream turbine arrays. This paper presents the results of CFD simulations of single turbines, modelled using a porous momentum loss (actuator disc), across a range of Coefficient of Thrust (C_T) values.

The CFD results are compared to experimental results which are disseminated in [1]. The purpose of the study is to demonstrate that the wake generated by a CFD simulation of an actuator disc has similar characteristics to experimental data obtained from porous discs across a range of C_T values. Comparisons within the CFD simulations give an indication of the quality of the model, and the parameters used.

2 Background

2.1 Simulating Turbines with Porous Discs in Experiments

Porous discs have been used by a number of authors to simulate the effect of a turbine on a fluid flow (either air or water) [1-3]. Actuator disks are beneficial at small scale where a number of scaling issues preclude the use of a small-scale rotating turbine. Under typical laboratory conditions (e.g. the Chilworth Flume at the University of Southampton, where the water depth is 0.3 m) a scaled turbine would need to have a diameter of around 0.1 m to give a reasonable representation of full-scale conditions. At this diameter the rotor would rotate at 1500 RPM to be scaled to a 10 m turbine at 15 RPM. This is not feasible from an engineering perspective, and moreover this rotational speed would introduce swirl and pressure gradients into the wake that would not be found under full-scale conditions [1].

It is therefore desirable to simulate the energy extraction and flow effects of a turbine more simply. The porous disc does this but has three key differences from a real turbine.

- Instead of extracting energy from the flow the porous disc converts it into small-scale turbulence immediately downstream.
- Vortices shed from the edges of the disc are different from those of a bladed turbine.
- The disc will not introduce any swirl into the flow, unlike a rotating blade.

The wake approximately 4D downstream has been shown to have a similar structure to that of a rotating turbine as most of the energy associated with swirl components has been dissipated. This is further discussed in [1-3]. However, swirl in the near wake can persist further downstream [4] potentially interacting with local flow boundaries causing the wake to meander. For simplification and to compare with experiments, the secondary effect of swirl has not been taken into account in this study.

This approach to simulating turbines has been adopted by Myers *et al.* [1, 5] and Sun *et al.* [6] for tidal devices. The method has also been used in wind tunnels [7, 8] for simulating wind turbines. Since the current studies are concerned ultimately with wake effects within turbine arrays, the flow at less than 4D downstream is unlikely to be of great interest. In wind turbine farms devices do not tend to be spaced at less that 7D apart due to a number of factors, including adverse turbulence effects [9], and this is likely to be the case for tidal devices.

It is useful to be able to vary the C_T of the porous disc, to study different turbines. This is done by varying the porosity of the mesh or plate used. The C_T of a turbine is defined by equation (1).

$$C_T = \frac{T}{0.5\rho {U_0}^2 A_d} \tag{1}$$

Equation (2) defines thrust in terms of the pressure drop across the disc/turbine. C_T may therefore also be defined by equation (3).

$$T = \Delta p A_d \tag{2}$$

$$C_T = \frac{\Delta p}{0.5\rho {U_0}^2} \tag{3}$$

Some attempts have been made to define a relationship between the porosity of the material and the resulting C_T *[10, 11]*. The material may be defined as having a drag coefficient, *K*, which relates the pressure drop across the disc with the velocity at the disc location – equation (4).

$$\Delta p = 0.5\rho K {U_d}^2 \tag{4}$$

Taylor [10] proposed a relationship between the open area ratio θ (a measure of porosity) and *K* as shown in equation (5). Whelan [11] examined this relationship and found that, while there is no clear theoretical basis for the model it gives a reasonable indication of *K* for a given *θ*.

$$\theta^2 = \frac{1}{1+K} \tag{5}$$

Taylor also gives a theoretical relationship between K and C_T. Equation 6 [10].

$$C_T = \frac{K}{(1+0.25K)^2} \tag{6}$$

It is essential that the C_T is measured (using a load cell etc.) for experiments involving porous disc simulators rather than derived theoretically. This was the case for the experimental data used in the present study. However when modelling a turbine in CFD it is necessary to better understand its resistance coefficient, as described below.

2.2 Simulating Turbines with a Momentum Loss in CFD Simulations

Similar to the concept of a porous disc for experimental studies, a momentum loss across a disc area in a CFD simulation also has a number of advantages. While the scaling issues do not apply to CFD (since the model may be specified at any dimensions) there are significant computational benefits in approximating the turbine as a disc rather than modelling its geometry in full. A full model of the turbine blades requires mesh resolution at the surface to be sufficient to capture the boundary layer and separation around the turbine, whilst also capturing the development of the wake up to 30D downstream. This requires a very large number of mesh elements (as seen in simulations by Mason-Jones [12]) and subsequently significant computational effort. Extending this meshing to multiple devices in array is not feasible with the modest resources available. Therefore the 'momentum loss disc' becomes a useful concept.

In an experiment the porous disc generates small-scale turbulence through the mesh, instead of extracting energy from the flow, while larger turbulence structures are generated from the disc edges. In a RANS CFD model turbulence kinetic energy is produced at areas of high velocity gradient, but the modelled disc structure will not generate mesh induced small scale turbulence unless it is designated as a source of turbulence kinetic energy. The level of ambient (free stream) turbulence has been noted as the primary factor affecting the rate of far wake recovery [1], and therefore in the present study mesh induced turbulence was not fully represented.

This method has been used for modelling tidal energy extraction by a number of authors including Batten & Bahaj [13], Sun *et. al.* [6] and Gant & Stallard [14]. While Sun provides some limited validation against experimental results of the wake produced by this CFD methodology [15] (at 3 D and 4 D downstream), other detailed studies of the accuracy of this method could not be found. Properly understanding and validating CFD results requires uncertainty analysis across a range of factors (described in detail by Marnet [16]), and this paper is a preliminary study of some of these.

In the current study the commercial CFD code Ansys CFX is used [17]. To define a porous region or momentum loss a sub-domain is defined across the disc mesh-volume. Within this sub-domain region a momentum 'source' is defined with a directional loss model based on a generalized form of the Darcy-Weisbach equation (equation 7).

$$S = \frac{\Delta p}{\Delta x_i} = \frac{K}{\Delta x_i}\frac{\rho}{2}U_d^{\ 2} \qquad (7)$$

Within CFX the resistance coefficient is entered as a gradient across the disc thickness, $K/\Delta x_i$. The momentum source defined by equation (7) is then added to the momentum equation of the Navier-Stokes equations within the CFD solver.

In order to run the model for the same values of C_T as found experimentally the correct value of K must be derived. Whelan [11] provides some experimentally derived values of K which can be used to investigate the results of the CFD model (Table 1).

For the CFD models presented in this paper, K was estimated using equation 6 and iterated to get values of C_T close to those presented in the experimental results for comparison.

θ – Open Area Ratio	0.58
K – measured resistance coefficient	~2
$K/\Delta x_i$ at $\Delta x_i=0.001m$	~2000
Estimated C_T calculated with equation (6)	0.88
Actual C_T in simple CFD model with $K/\Delta x_i$=2000	0.82

Table 1: Comparison of estimated C_T (using equation 6) and modelled C_T (uses data from [11])

3 Methodologies

3.1 Experimental Method

The experiments were carried out in a circulating water channel at the University of Southampton measuring 21m in length, 1.37 m wide running at a water depth of 0.3 m. A number of 0.1m-diameter discs of varying porosity were tested. Water velocities were measured at locations downstream using an Acoustic Doppler Velocimeter (ADV). Velocities in 3 planes were acquired at many locations at a sample rate of 50Hz. Mean sample time at each location was in the order of 3 minutes. The thrust on the disc was measured by installing the disc on a pivot arm mounted onto a load cell as shown in Fig 1.

3.2 Numerical Method

The numerical simulations were made using Ansys CFX 11 [17] which solves the Navier-Stokes mass and momentum equations. CFX uses a hybrid of the finite volume and finite difference discretization methods, allowing it to solve any mesh topology.

Previous CFD studies that applied the actuator disc method for modelling tidal turbines, such as those mentioned earlier in this paper, utilized the k-ε turbulence model within the RANS simulation. Preliminary simulations for the current study, together with work presented by Harrison *et. al.* [18] indicate that this turbulence model does not accurately model the flow conditions found in this scenario, and the k-ω SST (Shear Stress Transport) turbulence model was used. The rationale for this selection is that the SST model is known to perform well in situations with adverse pressure gradients, and separated flow [19]. Similar flow conditions would be present around an actuator disc, or a turbine.

The model domain was defined with similar dimensions to the experimental flume. A 2 m inflow, with the 0.1 m diameter disc located at the centre of a 0.3 m water column and a 3 m outflow. A symmetry plane ran down the XY centre plane through the disc - since the flow is identical either side – significantly reducing the model size and computational time. A free surface was modelled at 0.3 m water depth, with 0.15 m air modelled above. The width was 0.685 m, equivalent to half the width of the flume used for the experiments.

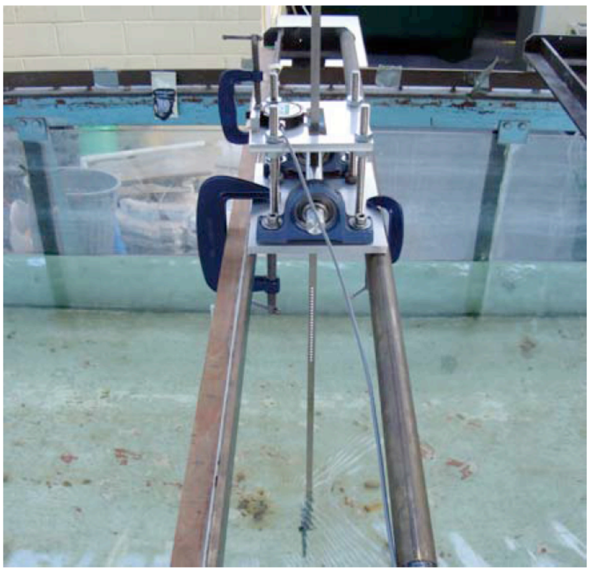

Fig. 1: Showing porous disc mounted on a pivot arm and load cell.

3.3 Numerical Boundary Conditions

The velocity at the inlet boundary was defined by curve fitting the Dyer boundary layer model (equation 8) [20] to measured inflow data from the experiments. Curve fitting supplied values of U^* and A, and the model was entered as an Ansys CFX CEL expression for the inlet boundary.

$$U_I = 2.5U^* \log\left(\frac{yU^*}{\nu}\right) + A \tag{8}$$

The turbulence at the inlet boundary was defined in terms of the turbulent kinetic energy (k), and eddy dissipation (ε), which were calculated from the measured turbulence intensity and velocity using equations (9) and (10).

$$k = \frac{3}{2} I^2 U^2 \tag{9}$$

$$\varepsilon = \frac{k^{3/2}}{0.3D_h} \tag{10}$$

The modelled inlet velocity and turbulence profiles are shown against the measured points in Fig. 2. The model values are taken at 1 m downstream of the inlet condition. It can be seen that modelled inflow velocity provides a reasonable match with experiments but turbulence intensities did not persist at the same values downstream. This is possibly due to the base of the tank not being a smooth wall and this requires further investigation.

To define the outflow condition an estimate of the free surface drop across the disc was made using momentum theory. This head loss was subtracted from the hydrostatic pressure at the outlet.

The top was defined as an opening with zero relative pressure and zero turbulence gradients. The bottom and outside wall of the flume were defined as smooth walls. The central plane was defined as a symmetry plane. The model parameters are summarised in Table 2.

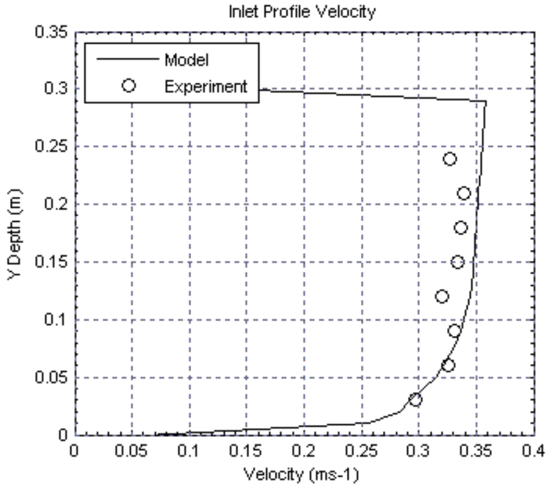

Fig. 2a: Modelled and measured inflow velocities

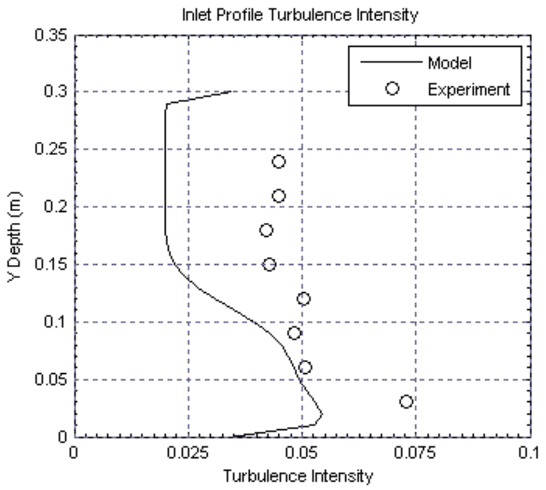

Fig. 2b: Modelled and measured inflow turbulence intensities.

3.4 Mesh adaptation study

A basic structured mesh was developed, with around 8.5 x 10^5 nodes. This mesh had sufficient nodes in the boundary layer to give $y+ < 100$, which is suitable for the SST turbulence model. The Ansys CFX mesh adaption system was used to increase the mesh density based on velocity gradients over 3 iterations. A node factor of 2.5 was applied which increased the final mesh to around 2.3 x 10^6 nodes – placed in areas where the velocity gradients are highest. The interim steps demonstrate any trend the model parameters may have which is dependent on the mesh density. To check for

Parameter	Setting
Water	Incompressible fluid
Air	Ideal Gas
Multiphase Control	Homogenous coupled free surface
Turbulence Model	SST
Inlet	Boundary layer model for velocities, experimentally derived k and ε. See Fig. 2.
Bottom and Outside Wall	No Slip Condition – Smooth Wall
Disc Centerline XY Plane	Symmetry
Outlet	Static pressure 0 Pa, Free surface height 0.3 m – 0.0012 m
Top	Opening, Air, 0 Pa
Convergence criteria	RMS residual 1 x 10^{-6}

Table 2: CFD Model Parameters

mesh independence the modelled C_T was compared across the 4 meshes, as well as the velocity profile at 7D downstream of the disc. The solution appeared to be mesh independent in most parameters.

Fig. 3 shows a sample of the mesh structure after adaption. Table 3 shows the trend of C_T values across the 4 meshes at 5 C_T values. Fig. 4 shows the velocity at 7D downstream of a disc with $C_T = 0.83$.

4 Results & Discussion

Where velocities are compared between model and experiments they are normalised using the average of the inflow velocity for $0.05 \leq y \leq 0.25$ m. This is because no measured data exists below 0.03 m depth, or above 0.24 m.

Figs. 5 a-d compare the modelled flow behind a disc of $C_T = 0.83$ and experimental data for a disc of $C_T = 0.8$ in centreline XY and XZ planes.

Figs. 6a and 6b show contour plots of the velocity and Figs. 6c and 6d the turbulence kinetic energy in an XY slice behind a modelled disc of $C_T = 0.83$, and measured behind a disc with $C_T = 0.8$.

Figs. 7a and 7b show the centreline velocity, and turbulence intensity behind discs of varying C_T for both models and experiments.

Observations: Model Boundary Conditions

Fig. 2a confirms that the modelled inlet velocity profile was well matched with the experiments. The velocity increases between $0 \leq y \leq 0.1$ m, and is fairly constant above this depth.

The turbulence profile (Fig. 2b) is not as well matched. While the free stream modelled values were identical to the measured values at the inlet, they dissipate downstream. Figs, 5b and 5d indicate that at the disc location, and further downstream the free stream turbulence values are more closely matched. Throughout the model, below 0.1 m depth the inlet turbulence levels are also better matched. Boundary layer development in the model may have caused the improved agreement below 0.1 m depth, and further downstream.

Further investigation of the inflow length and conditions are required to resolve this and ensure a good match of ambient turbulence levels for future modelling.

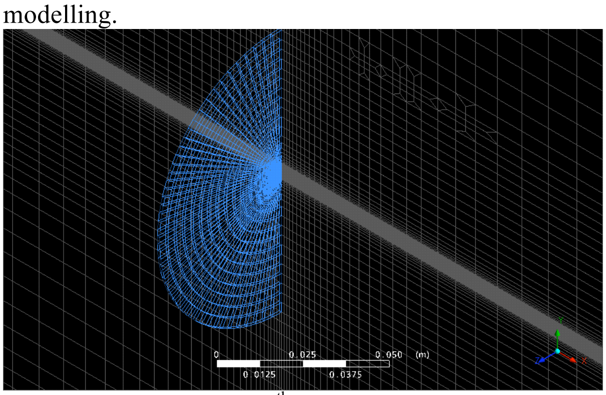

Fig. 3: Structured mesh at 4th adaption level, disc is shown in the centre of the image.

Number of Nodes in Mesh	Value of $K/\Delta x_i$				
	1000	1500	2000	2500	3000
8.5E+05	0.576	0.712	0.810	0.884	0.942
1.3E+06	0.588	0.726	0.826	0.902	0.959
1.8E+06	0.587	0.725	0.826	0.921	0.960
2.3E+06	0.585	0.725	0.825	0.903	0.959

Table 3: Showing variation in C_T as a function of K and number of mesh nodes.

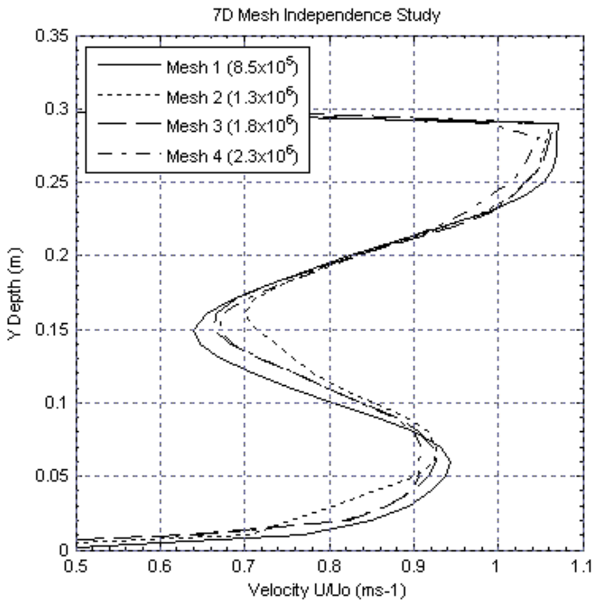

Fig. 4: Variation in the velocity (ms^{-1}) with mesh density 7D downstream of a disc with $C_T = 0.83$

Observations: Model/ Experiment Agreement at $C_T = \sim 0.8$

At $C_T = \sim 0.8$ the model gives reasonable agreement with the experimental results. The main points of agreement were:

- The fluid was faster flowing above the disc, ($y > 0.2$m) than below ($y < 0.1$ m) – Fig. 5a.
- The slow moving wake recovered to around 0.9 of the free stream velocity at 20D downstream - Figs. 5a, 6a & b.
- At the centreline the velocity falls to around 0.45 of free stream at 4D downstream – Figs. 5a, 6a & b.
- The free stream turbulence levels (i.e. $Z > 0.1$ m) were well matched on the centreline XZ plane - Fig. 5d.

The main discrepancies between model and experiment were:

- Modelled turbulence values in the wake region were much lower than the experimental values (Figs. 5b, 5d, 6c & 6d). As mentioned above the modelled disc does not induce any turbulence in the flow, while a mesh disc simulator does. The

low turbulence intensity immediately behind the disc is clearly shown in Fig. 6c compared to 6d.
- At 7D downstream agreement in the depth-wise velocity profiles is inadequate (Fig. 5a). The experimental wake recovers faster than the modelled wake. Wake recovery is dependent on free stream turbulence entraining energy back into the slow moving wake fluid. Since the free-stream turbulence in the model was lower than the experiments this would explain why the rate of recovery was slower for the model (Fig. 6c and 6d).
- The experimental results show that the wake is centred below the centre of the disc – with the lowest velocity values occurring a little below the disc centreline. It has been postulated that this is caused by a unequal mass flow rate above and below the disk caused by the shape of the vertical velocity profile [1]. More flow above the disk pushes the wake structure downwards. While the model results show similar flow speed characteristics above and below the disc ($y < 0.1$ and $y > 0.2$) this has not caused the same realignment of the wake structure.

Observations: Model/Experiment Agreement Across Range of C_T

Across the range of C_T values that were modelled similar agreement to the $C_T = \sim 0.8$ case was demonstrated. The results are not shown in full here due to space constraints.

Myers *et al.* [1] notes that C_T has an affect on the initial drop in velocity in the wake, but as the wake recovers the centreline velocity values converge. This is because wake recovery is largely driven by free-stream turbulence which is unaffected by C_T.

This effect was replicated in the models (Fig. 6a). The experimental values are separate up to around 6D downstream, but then converge. A similar effect was noted for the models, with the $C_T = 0.7$, $C_T = 0.83$ and $C_T = 0.96$ cases converging around 6D downstream.

The initial deficit and rate of recovery were different between models and experiments. The initial deficits were lower for the models, and rate of recovery was slower. As mentioned above the slower rate of recovery can be attributed to lower ambient turbulence intensities in the models. The lower initial velocity deficit may be caused by the lack of turbulence generated by the modelled disc – which could entrain some energy from the free stream fluid at this location close to the disc. Figs. 6(c, d) clearly shows the difference in wake turbulence intensities between model and experiment.

5 Conclusions

Comparison of the model and experiment results demonstrates the applicability of the CFD modelling methodology, and some of the key factors that affect its accuracy. The main findings were:

CFD Parameters:

- Robust boundary conditions were used. The Dyer boundary layer model gave a good estimation of the measured inflow velocity. Estimation of the head loss across the disc provided a suitable outlet pressure for the model. The turbulence levels dissipated away from the inflow boundary; further work is required to ensure this is better matched in the model.
- A mesh independent model was developed and it was found that 1.3×10^6 nodes gave similar results across most values, in terms of C_T and velocity profiles, to a mesh of 2.3×10^6 nodes. This may be exploited to reduce computational time in future modelling.

Comparison of Model and Experimental Results

The main points of agreement were:
- Across the range of C_T values the model results followed the same trend as the experimental results, converging around 6D downstream of the disc.
- The wake recovered to around 0.9 of free stream velocity at 20D downstream.
- The free stream turbulence levels on the central XZ plane were similar indicating that the boundary layer was not as well developed in the model as in the experiments.

The main differences between the experiment and model results were:
- The initial velocity deficit for a specific C_T was higher for the model than the experiments.
- The turbulence levels in the wake were much lower for the model results, since the modelled disc was not a source of turbulence. This may be the reason for the higher initial velocity deficits
- The wake recovery was more rapid for the experimental results. This was caused by lower modelled ambient turbulence intensity.

Further Work

The results presented in this paper will inform further modelling, with particular emphasis on matching inflow turbulence intensities and a more realistic approximation of the wake including swirl effects.

Acknowledgements

This modelling work is funded by the EPSRC under the Supergen Marine research program. The experimental work was part of a UK Technology Strategy Board-funded project ‘Performance characteristics and optimisation of marine current energy converter arrays”, project number T/06/00241/00/00

References

1. Myers, L. E., Bahaj, A.S., Thomson, M. D., Jorge, N. Characterisng the Wake of Horizontal Axis Marine Current Turbines. in Proceedings Seventh European Wave and Tidal Energy Conference. 2007. Porto.

2. Connel, J.R. and R.L. George, The wake of the MOD-0A1 wind turbine at two rotor diameters downwind on 3 December 1981. 1982, Pacific Northwest Laboratory: Battelle, US.

3. Vermuelen, P.E.J., Mixing of simulated wind turbine wakes in turbulent shear flow. 1979, TNO.

4. Troldborg, N., J.N. Sorensen, and R. Mikkelsen, Actuator Line Simulation of Wake of Wind Turbine Operating in Turbulent Inflow Journal of Physics: Conference Series, 2007. 75.

5. Myers, L.E., Bahaj, A. S., Rawlinson-Smith, R., Thomson, M. The effect of boundary proximity upon the wake structure of horizontal axis marine current turbines. in Proceedings 27th International Conference on Offshore Mechanics and Arctic Engineering (OMAE 2008). 2008. Estoril, Portugal.

6. Sun, X., J.P. Chick, and I.G. Bryden, Laboratory-scale simulation of energy extraction from tidal currents. Renewable Energy, 2008. 33: p. 1267-1274.

7. Sforza, P.M., P. Sheerin, and M. Smorto, Three-dimensional Wakes of Simulated Wind Turbines. AIAA Journal, 1981. 19(9): p. 1101-1107.

8. Builjtes, P.J. The interaction of windmill wakes. in Second International Symposium on Wind Energy Systems. 1978. Amsterdam.

9. Crespo, A., J. Hernandez, and S. Frandsen, Survey of Modelling Methods for Wind Turbine Wakes and Wind Farms. Wind Energy, 1999. 2: p. 1-24.

10. Taylor, G.I., The scientific papers of Sir Geoffrey Ingram Taylor, ed. G.K. Batchelor. 1963: Cambridge University Press.

11. Whelan, J., Thomson, M. Graham, J. M. R, Peiro, J. Modelling of free surface proximity and wave induced velocities around a horizontal axis tidal stream turbine, in Seventh European Wave and Tidal Energy Conference. 2007: Porto, Portugal.

12. Mason-Jones, A., O'Doherty, T., O'Doherty, D. M., Evans, P. S, Wooldridge, P. S. Characterisation of a HATT using CFD and ADCP site data. in Proceedings World Renewable Energy Congress (WREC-X). 2008. Glasgow.

13. Batten, W.M.J. and A.S. Bahaj. CFD simulation of a small farm of horizontal axis marine current turbines. in Proceedings World Renewable Energy Congress (WREC-IX). 2006. Florence.

14. Gant, S. and T. Stallard. Modelling a Tidal Turbine in Unsteady Flow. in Proceedings International Society Offshore and Polar Engineers. 2008. Vancouver.

15. Sun, X., Numerical and Experimental Investigation of Tidal Current Energy Extraction. 2007, University of Edinburgh: Edinburgh.

16. MarnetCFD, Best practice quidelines for marine applications of compuatational fluid dynamics. 2003, WS Atkins.

17. Ansys, Ansys CFX. 2007.

18. Harrison, M.E., Batten, W. M., Bluden, L. S., Myers, L. E., Bahaj, A. S., Comparisons of a Large Array of Tidal Turbines Using teh Boundary and Field Wake Interaction Models, in Second International Conference on Ocean Energy. 2008: Brest, France.

19. Menter, F.R., A comparison of some recent eddy-viscosity turbulence models. Journal of Fluids Engineering, 1996. 118: p. 514.

20. Dyer, K., Coastal and Estuarine Sediment Dynamics. 1986: John Wiley and Sons. 358.

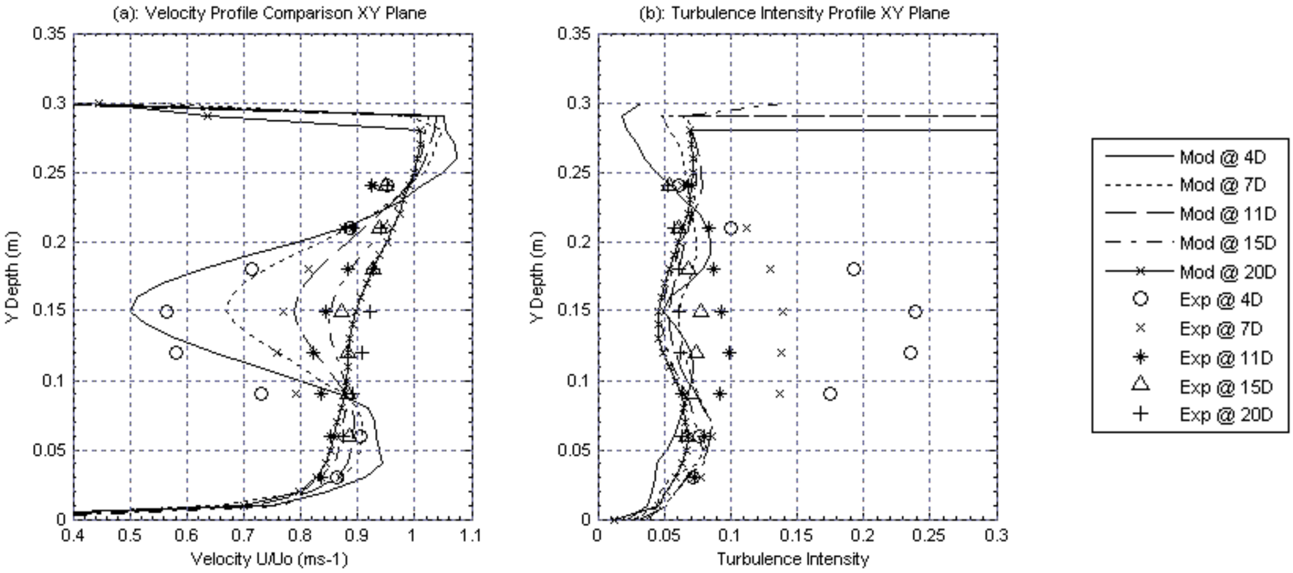

Fig. 5a and 5b: Relative velocity (u/Uo) in XY centreline plane behind disc with modelled C_T = 0.83 and measured C_T = 0.8.

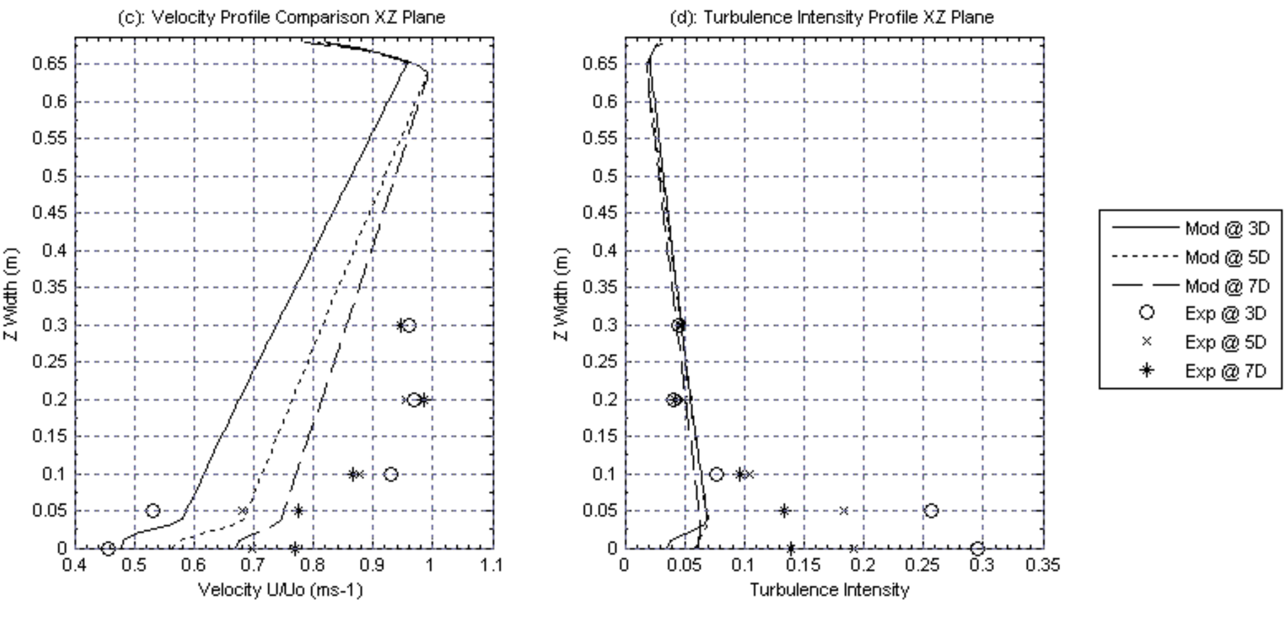

Fig. 5c and 5d: Relative velocity (u/Uo) in XZ centreline plane behind disc with modelled C_T = 0.83 and measured C_T = 0.8.

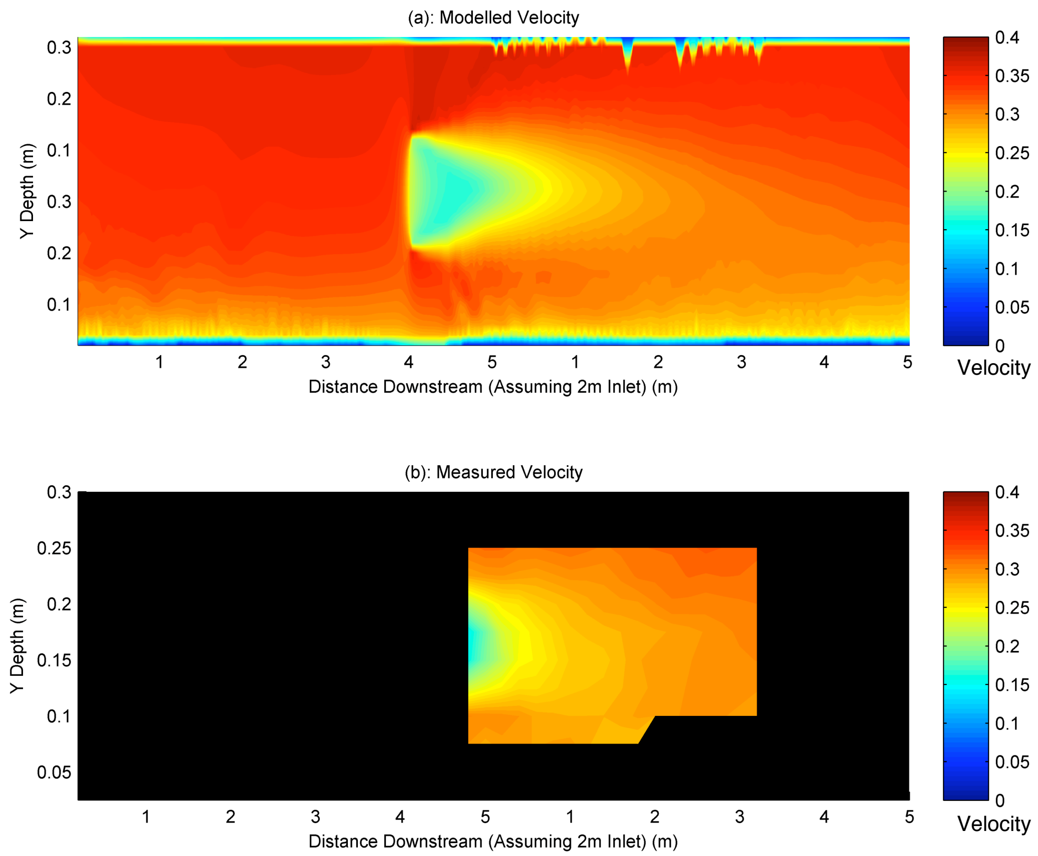

Fig. 6a: Stream-wise velocities behind a modelled disc $C_T = 0.83$.

Fig. 6b: Stream-wise velocities measured behind a disc $C_T = 0.8$.

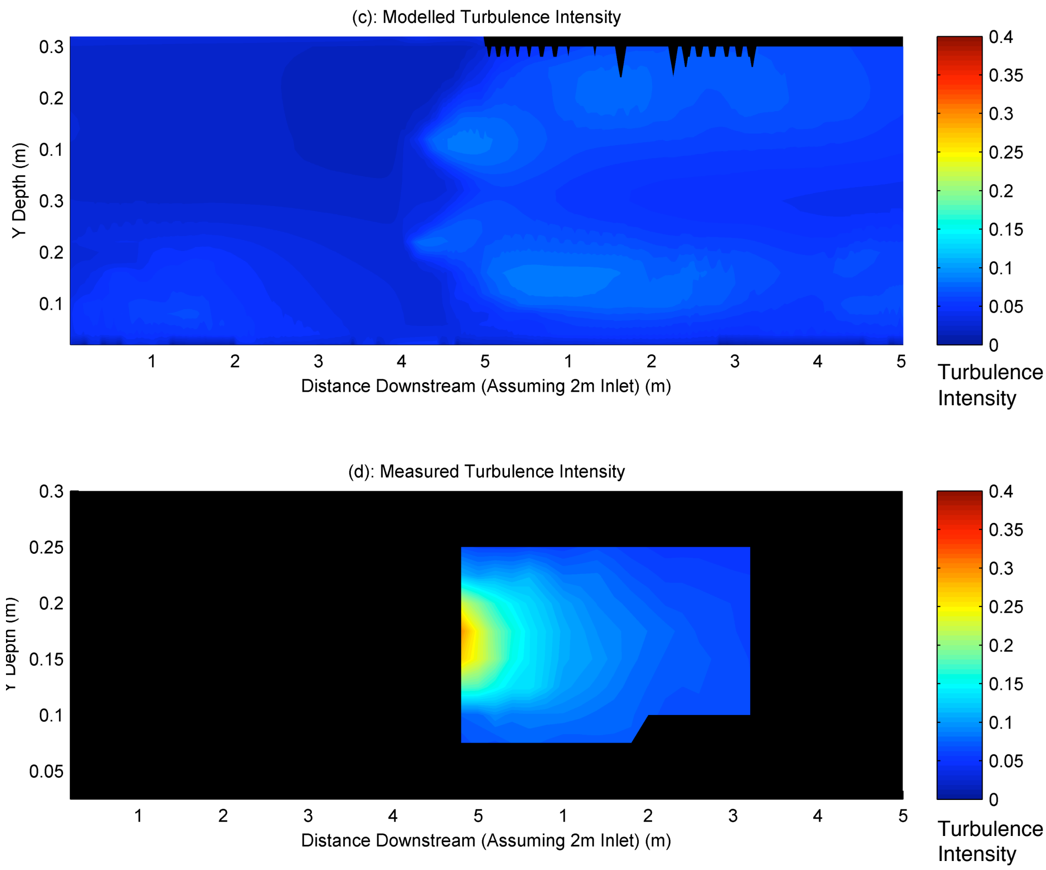

Fig. 6c: Turbulence intensities behind a modeled disc $C_T = 0.83$.

Fig. 6d: Turbulence intensities measured behind a disc $C_T = 0.8$.

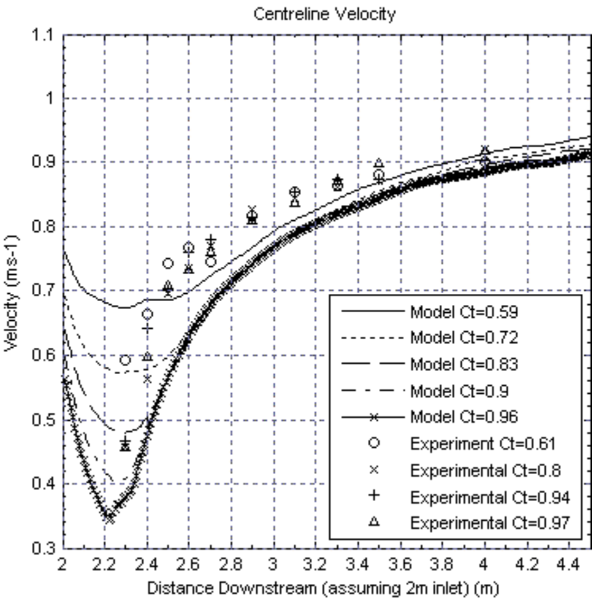

Fig. 7a: Centre-line velocity as a function of distance downstream and disc C_T

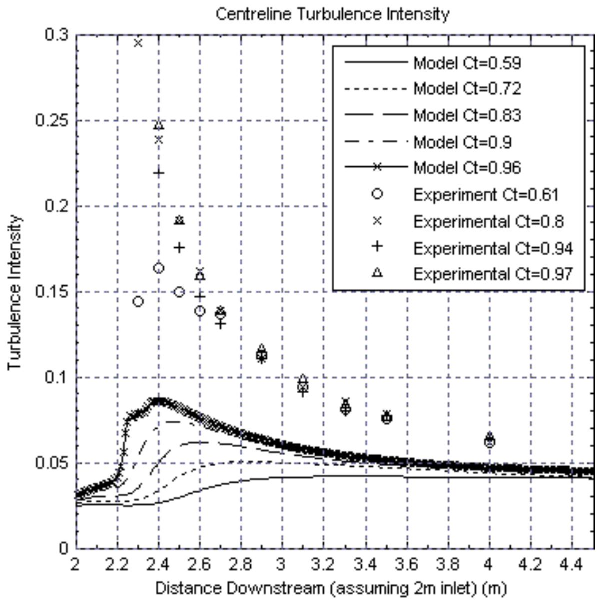

Fig. 7b: Centre-line turbulence intensity as a function of distance downstream and disc C_T